EXPERIMENTAL STUDY ON SEISMIC BEHAVIOR AND CRACK PATTERN OF CONCRETE BLOCK INFILLED RC FRAMES

YOSHIAKI NAKANO
Institute of Industrial Science, The University of Tokyo, Tokyo, Japan
iisnak@iis.u-tokyo.ac.jp
HO CHOI
Graduate School of Engineering, The University of Tokyo, Tokyo, Japan
choiho@iis.u-tokyo.ac.jp

ABSTRACT

In this study, concrete block infilled reinforced concrete frames for school buildings in Korea are tested under cyclic loadings, and a simplified model is proposed to investigate the relationship between residual crack widths in concrete block wall and frame's residual deformations. Although the measured crack widths in concrete block walls are much smaller than the residual deformations, a simplified model proposed in this paper considering flexural and shear deformation distribution of columns can rationally reproduce the measured crack widths. The relationship between crack widths in concrete block wall and frame's residual deformations is further investigated and their ratio is found to lie approximately in the range of 0.2 to 0.3. This result implies that the residual deformation of frames can be estimated form crack widths in concrete block wall.

1. INTRODUCTION

After an earthquake, the major concerns to damaged buildings are their safety/risk to aftershocks, quantitative damage assessment to evaluate their residual seismic capacity and to identify necessary actions on the damaged buildings. Post-event damage evaluation is therefore essential for quick recovery of damaged communities as well as pre-event seismic evaluation and strengthening of vulnerable buildings. Few investigations on unreinforced masonry walls, however, have been made to quantitatively identify their damage level and criteria to judge necessary actions for their continued use, repair and rehabilitation although their damage has been often found in the past damaging earthquakes.

In this study, concrete block (CB) infilled RC frames for school buildings in Korea, where CB walls are typically unreinforced, are experimentally investigated to develop pre- and post-earthquake seismic evaluation method. In the tests, full-scale, one-bay, single-story specimens having different axial loads in columns and different opening configurations in walls are tested under cyclic loadings, and the contribution of CB walls to overall behaviors is examined. Furthermore, crack patterns and widths in walls and frames which may be of great significance for post-event damage assessment are carefully observed, and the measured results in CB wall are compared to those estimated by a simplified model proposed in this paper.

2. OUTLINE OF EXPERIMENT

2.1 Test Specimen

Figure 1 shows a standard design for Korean school buildings in the 1980s (The Ministry of Construction and Transportation, 2002). As can be found in this figure, CB walls are commonly used as partition walls or exterior walls in Korean school buildings. In this study, 4 specimens representing a first or fourth story of 4 story RC school buildings are tested under cyclic loadings. They are infilled wall type 1 (IW1) assuming a first story, infilled wall type 2 (IW2) assuming a fourth story, and wing wall type (WW) and partial height wall type (PW) both having an opening in the wall. The axial force applied in each column is 720 kN (4 N/mm^2) for specimens IW1, WW, and PW while 180 kN (1 N/mm^2) for IW2.

The design details of specimen IW1 are shown in Figure 2. Since seismic design provisions for buildings were introduced in 1988 in Korea, the model structures studied herein are not designed to seismic loads. Therefore, they have (1) large spacing of hoops (300 mm) and (2) 90-degree hooks at both ends of hoops as shown in the figure. Specimens IW1, WW,

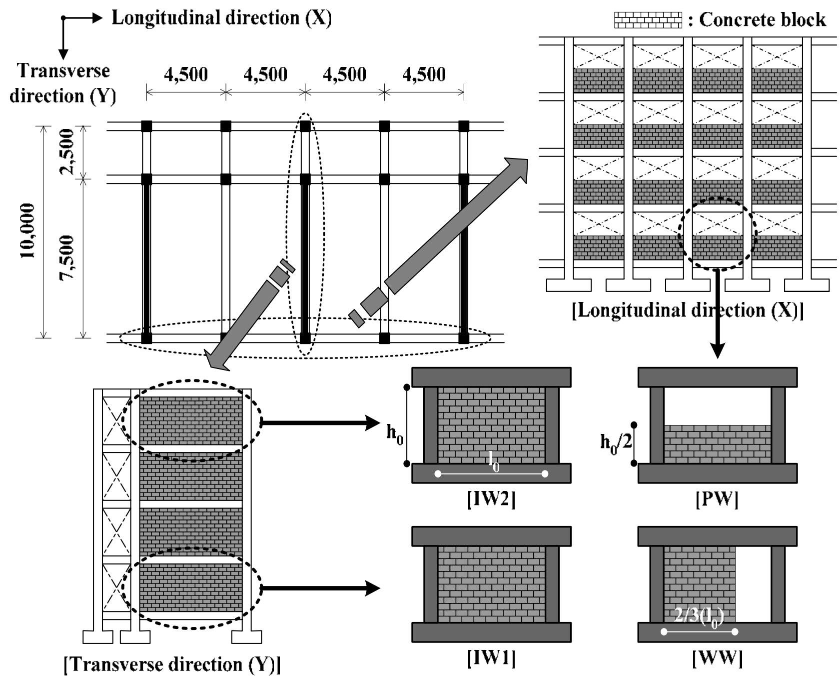

Figure 1: Standard design of Korean school buildings in the 1980s and specimen configuration

and PW have the identical re-bar arrangement in columns but different wall arrangement, while IW2 has fewer re-bars than other 3 specimens. Concrete block units are laid in the RC frame after concrete is hardened.

2.2 Test Setup and Test Program

Figure 3 and Photo 1 show the elevation view of the loading system. Cyclic lateral loads are applied to each specimen through a loading beam tightly fastened to the specimen. Figure 4 shows the loading history, where a peak drift angle R is defined as "lateral deformation (δ_p) / column height (=2,400 mm)". As shown in the figure, peak drift angles of 0.1, 0.2, .0.4, 0.67, 1.0, and 2.0% are planned and 2.5 cycles for each peak drift are imposed to eliminate one-sided progressive failure (unsymmetric failure pattern in positive or negative loadings). It should also be noted that 0.4% loading is imposed after 1.0% to investigate the effect of small amplitude loading after large deformation (i.e., aftershocks). After severe damage is found, the specimen is pushed over to collapse. A constant axial load of 1,440 kN (720 kN for each column) is applied to specimens IW1, WW and PW while 360 kN (180 kN for each) to specimen IW2.

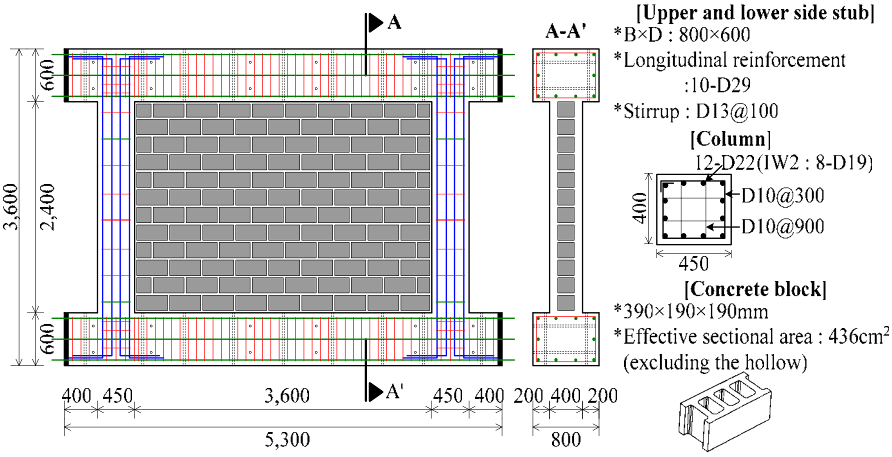

Figure 2: Detail of specimen (IW1)

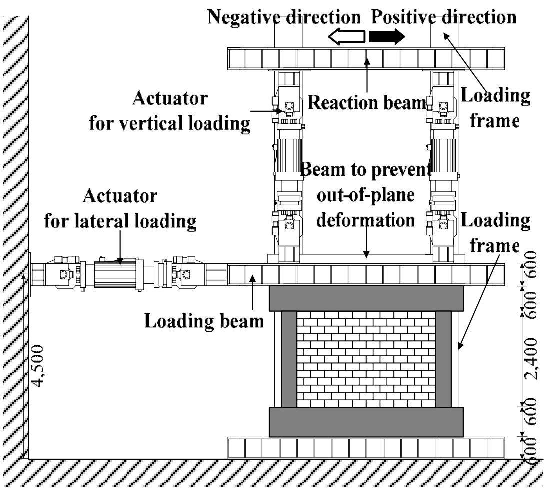

Figure 3: Test setup

Photo 1: General view of test setup

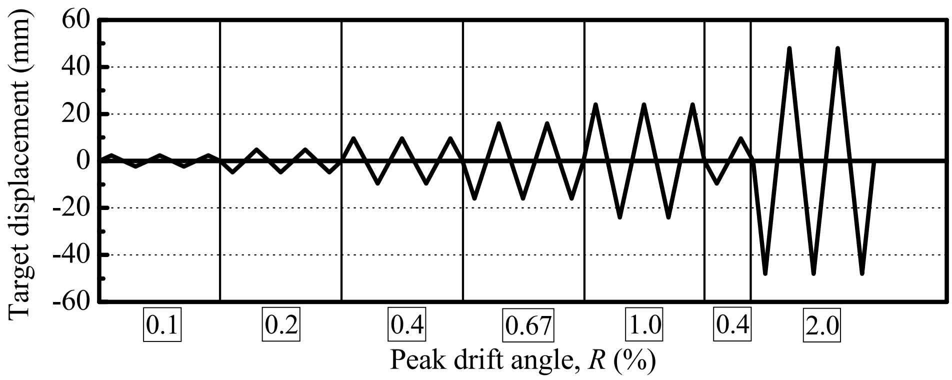

Figure 4: Loading history

3. CRACK WIDTHS AND RESPONSE OF SPECIMENS

3.1 Measurement of Crack Width

Cracks in members after an earthquake are visible and essential evidence of damage that can be found at the building site, and they often provide valuable information regarding the response that the building has experienced and its residual capacity. To investigate the relationship between crack width and residual capacity, crack widths in RC columns and CB walls are carefully measured at peak loads and unloaded stages. Figure 5 shows the measurement points in columns and walls made in this study.

The widths of flexural and shear cracks observed at the top and bottom of each column are visually measured with crack scales. Since crack widths are not necessarily uniform along the crack, its major width which is deemed to be largest along a crack is measured. It should also be noted that the width perpendicular to the crack is measured.

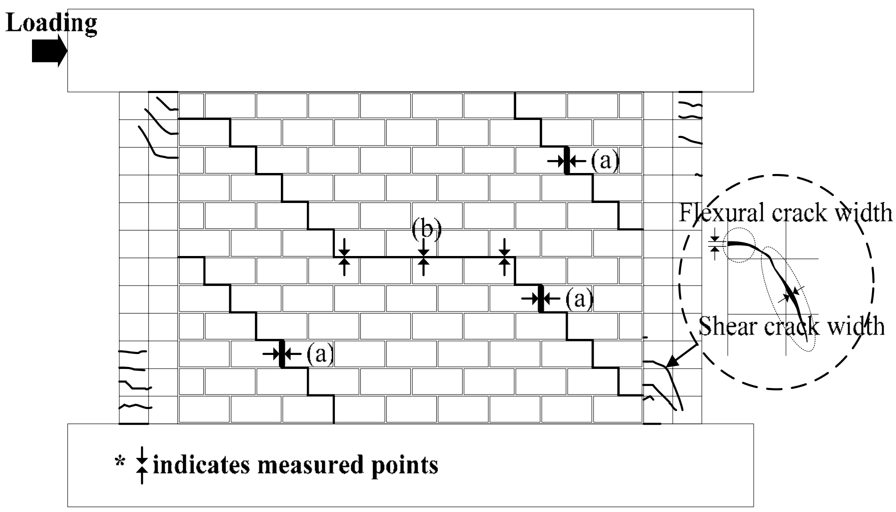

Figure 5: Schematic illustration of crack pattern and measured points

All visible cracks in the head joints found in stair-stepped diagonal cracks running through the CB wall are also measured to record the lateral dislocation of CB units (see Figure 5(a)) while several cracks in the bed joints of one continued crack are measured to investigate a rotational behavior of wall (see Figure 5(b)). In the following sections, crack widths measured in the head joints of CB walls of specimens IW1 and IW2 are investigated to understand the relationship between observed cracks and frame's behavior.

3.2 Residual Crack Width in CB Wall

The residual deformation (δ_0), total residual crack width ($\Sigma\ {}_{\max}W_0$) measured in CB wall, and their ratio [$\Sigma\ {}_{\max}W_0$ / δ_0] at unloaded stages after each first cycle in the positive domain are plotted for specimens IW1 and IW2 with respect to the peak drift angle in Figure 6. In this figure, ${}_{\max}W_0$ is defined as the maximum residual crack width, as is shown (a) in Figure 5, in the head joints of a continued stair-stepped diagonal crack. When the CB wall has more than one major stair-stepped diagonal crack, ${}_{\max}W_0$ can be found along each continued crack and the sum of ${}_{\max}W_0$ (= $\Sigma_{\max}W_0$) is then calculated. The ratio [$\Sigma\ {}_{\max}W_0$ / δ_0] of specimen IW1 differs from that of IW2 over the peak drift angle R smaller than 0.2% and larger than 1.5%. The results can be attributed to the following observations.

(1) The ratio tends to be dependent on crack inspectors especially when the deformation is small (i.e., $R \leq 0.2\%$) since the observed crack widths are around 0.1mm which would be the limit for visual inspections. The calculated ratio is therefore sensitive to the measurement error and may not be consistent in the small drift range along different specimens.
(2) The crack widths in CB wall significantly increases after R = 1.4% in IW1 due to extensive shear cracks in columns, while IW2 performs well even in such a large deformation. The ratio is therefore higher in IW1 than in IW2.

It should also be noted that the ratio [$\Sigma\ {}_{\max}W_0$ / δ_0] is approximately in the range of 0.2 to 0.3 over the peak drift angle larger than 0.2 % and much smaller than 1.0. The reason can be found in the following section.

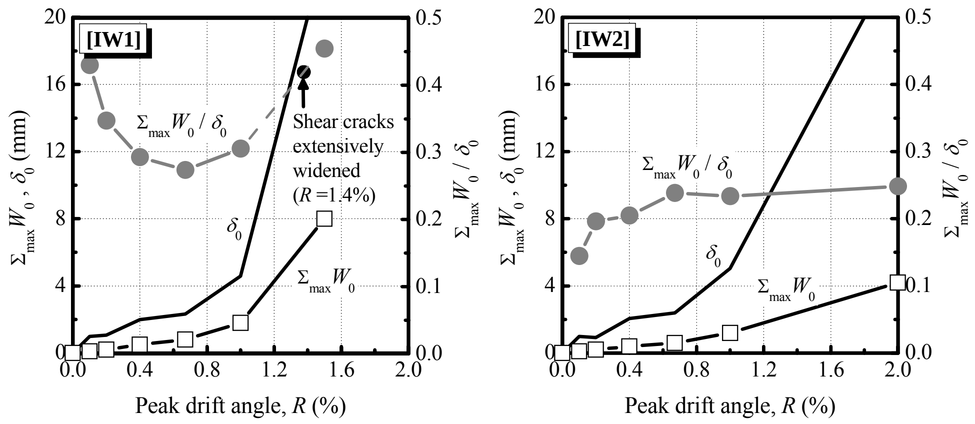

Figure 6: δ_0 , $\Sigma\ {}_{\max}W_0$ and [$\Sigma\ {}_{\max}W_0$ / δ_0] (CB wall) vs. peak drift angle R

3.3 Estimation of Measured Crack Width in CB Wall by Simplified Model

(1) General assumptions

In order to investigate the crack development mechanism and to estimate the crack width in CB wall, the following assumptions are made.

1) The residual deformation (δ_0) of frame can be approximated by the sum of residual flexural deformation (δ_{f0}) and residual shear deformation (δ_{s0}) of column as shown in Figures 7(a) and (b). (i.e., $\delta_0 = \delta_{f0} + \delta_{s0}$)
2) Cracks in head joints of CB wall result from the discrepancy of deformation distribution along its height in each column.

If each column has an identical anti-symmetrical flexural deformation and distribution as shown in Figure 7(a), no discrepancy should be found in the CB wall's clear span length l_{0i} along column height (i.e., $l_{01} \approx l_{02} \approx l_{03}$). Since a similar flexural deformation distribution is observed in each column during tests, no major cracks due to flexural deformation are expected.

The shear deformation distribution along its height in each column, however, is not obviously identical as shown in Figure 7(b), since the deformation due to shear cracks concentrates on the bottom of compression column and the top of tensile column resulting from a compressive strut action as can be found in specimens IW1 and IW2 (see Figure 8). This may cause the discrepancy of lateral deformation distribution in CB wall along

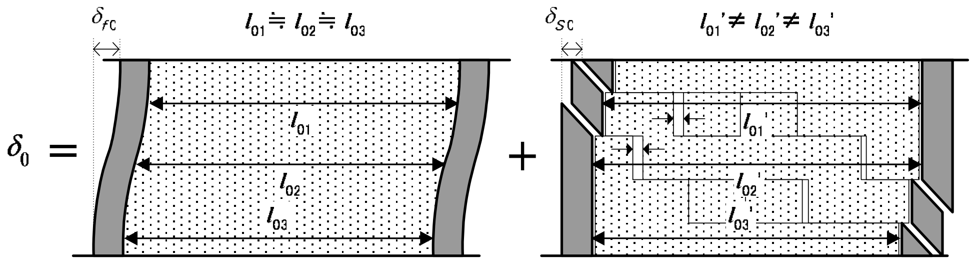

(a) Flexural deformation *(b) Shear deformation*

Figure 7: Deformation of column and CB wall

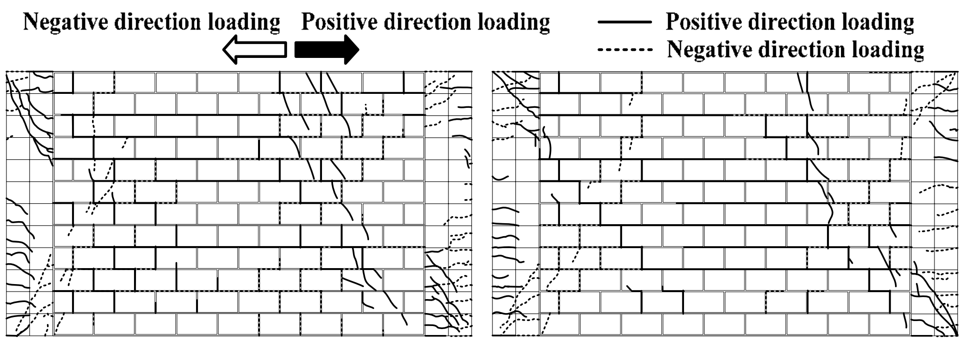

(a) IW1 *(b) IW2*

Figure 8: Cracks in RC columns and CB wall at the 1st cycle with peak drift angle of +1.0%

column height (i.e., $l_{01}' \neq l_{02}' \neq l_{03}'$). The maximum discrepancy, which may be simply expressed by the residual shear deformation (δ_{s0}) as shown in Figure 7(b), then needs to be consistent with crack widths in head joints resulting in high correlation between the residual shear deformation (δ_{s0}) and total crack width in CB wall ($\Sigma_{max} W_0$).

Bearing in mind that the flexural deformation may highly contribute to the overall deformation of long columns but that the flexural deformation, as is described earlier, may not cause major cracks in head joints, the ratio [$\Sigma_{max} W_0$ / δ_0] can be expected to be small as demonstrated in Figure 6. Based on studies by Maeda et al.(2000), AIJ Guidelines define the relationship between residual crack width and residual deformation for RC members (AIJ, 2004). However, few researches on the relationship for RC frames and/or CB wall infilled frames have been yet made to date. It is therefore of great interest and significance to investigate the applicability of analogous relationship to CB wall infilled frames. In the subsequent discussions, a simplified model considering the discrepancy of flexural and shear deformation distribution is proposed to estimate the crack width in CB wall, and the correlation between measured and estimated results is discussed.

(2) Crack width due to flexural deformation

Figure 9 shows the outline of the simplified model studied herein. The flexural deformation, ${}_t\delta_f$ and ${}_c\delta_f$, of each column can be approximated using the average total flexural crack width at the top and bottom of column as shown in equations (1) and (2) (AIJ, 2004), where "*t*" and "*c*" denote "tension side" and "compression side", respectively. The maximum discrepancy between two columns due to flexural deformation distribution, which causes minor cracks in head joints as discussed earlier, is assumed herein to develop in the mid-height of column ($h_0/2$) as shown in equation (3).

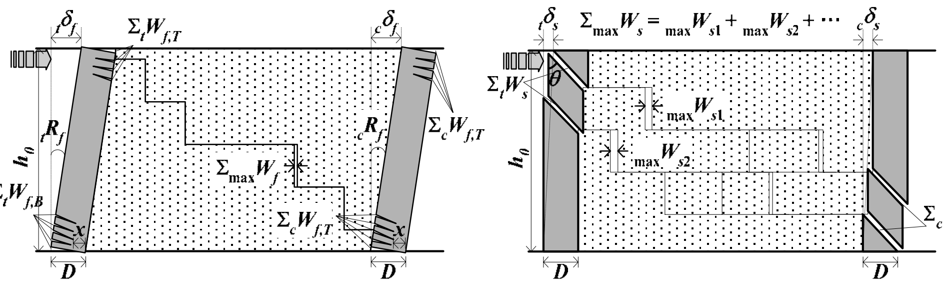

(a) Flexural deformation *(b) Shear deformation*

Figure 9: Simplified model of column and CB wall

$$ {}_t\delta_f = {}_tR_f \cdot h_0 = \frac{1}{D-x} \cdot \left(\frac{\Sigma_t W_{f,T} + \Sigma_t W_{f,B}}{2} \right) \cdot h_0 \tag{1} $$

$$ {}_c\delta_f = {}_cR_f \cdot h_0 = \frac{1}{D-x} \cdot \left(\frac{\Sigma_c W_{f,T} + \Sigma_c W_{f,B}}{2} \right) \cdot h_0 \tag{2} $$

$$ \Sigma_{max} W_f = \left(\frac{\Sigma_c W_{f,B} - \Sigma_t W_{f,B}}{D-x} \right) \cdot \frac{h_0}{2} \tag{3} $$

where,

${}_t\delta_f$, ${}_c\delta_f$	: flexural deformation of tension and compression side column, respectively (see Figure 9(a))
${}_tR_f$, ${}_cR_f$	: flexural rotation angle of tension and compression side column, respectively (see Figure 9(a))
$\Sigma_t W_{f,T}$, $\Sigma_t W_{f,B}$	: total flexural crack width of top and bottom in tension column, respectively (measured)
$\Sigma_c W_{f,T}$, $\Sigma_c W_{f,B}$	: total flexural crack width of top and bottom in compression column, respectively (measured)
D	: column depth (=450 mm)
x	: distance from extreme compression fiber to neutral axis ($0.2D$ (= 90 mm) is assumed herein)
h_0	: column clear height (= 2,400 mm)
$\Sigma_{max} W_f$	: total crack width in CB wall due to the discrepancy of flexural deformation distribution

(3) Crack width due to shear deformation

The shear deformation, ${}_t\delta_s$ and ${}_c\delta_s$, of two RC columns can be approximated based on the measured total shear crack width of each column as shown in equations (4) and (5) (AIJ, 2004). The total crack width in CB wall due to different shear deformation distribution between tension and compression side column can be estimated using the average total shear crack width as shown in equation (6).

$$ {}_t\delta_s = \Sigma_t W_s \cdot \cos\theta \tag{4}$$

$$ {}_c\delta_s = \Sigma_c W_s \cdot \cos\theta \tag{5}$$

$$ \Sigma_{max} W_s = \frac{{}_c\delta_s + {}_t\delta_s}{2} \left(= \frac{(\Sigma_c W_s + \Sigma_t W_s) \cdot \cos\theta}{2} \right) \tag{6}$$

where,

${}_t\delta_s$, ${}_c\delta_s$	: shear deformation of tension and compression side column, respectively (see Figure 9(b))
$\Sigma_t W_s$, $\Sigma_c W_s$	: total shear crack width of tension and compression side column, respectively (measured)
θ	: angle between shear crack and vertical direction of column (45-degree angle is assumed herein)
$\Sigma_{max} W_s$	: total crack width in CB wall due to the shear deformation distribution

(4) Total crack width in CB wall

As shown in equation (7), the total crack width in CB wall, $\Sigma_{max} W$, can be calculated using crack widths defined in equations (3) and (6).

$$ \begin{aligned} \Sigma_{max} W &= \Sigma_{max} W_f + \Sigma_{max} W_s \\ &= \left(\frac{\Sigma_c W_{f,B} - \Sigma_t W_{f,B}}{D - x} \right) \cdot \frac{h_0}{2} + \frac{(\Sigma_c W_s + \Sigma_t W_s) \cdot \cos\theta}{2} \end{aligned} \tag{7}$$

Figure 10 shows the residual deformation δ_0 and δ_{f0} with respect to the peak drift angle, where δ_{f0} is assumed to be the average of ${}_t\delta_f$ and ${}_c\delta_f$ at unloaded stages derived from equations (1) and (2). Since major wide cracks are selectively measured after 1.0 % drift, δ_{f0} is plotted up to 1.0 %. As is anticipated in 3.3 (1), δ_{f0} mainly contributes to the overall residual deformation δ_0. It is also interesting to point out that the ratio of crack widths $\Sigma_{\max}W_{f0}$ to δ_{f0} is relatively small, which is consistent with the results shown in Figure 6. This is mainly because the flexural deformation distribution along their height of two boundary columns does not differ much (i.e., $l_{01} \approx l_{02} \approx l_{03}$) and therefore leads to minor cracks in head joints.

Figure 11 shows the estimated crack widths in CB wall at unloaded stages obtained from equation (7) together with measured results. The estimated results (shown in circle : -○-) slightly overestimate the measured results (shown in square : -□-) since all cracks developed in CB wall are not perfectly measured during tests. The estimated results, however, generally compare well with the measured results and the proposed model shown in Figure 9 successfully explains the crack development mechanism of CB wall studied herein. This result implies that the residual deformation δ_0 of frames as well as RC members can be estimated from crack widths $\Sigma_{\max}W_0$

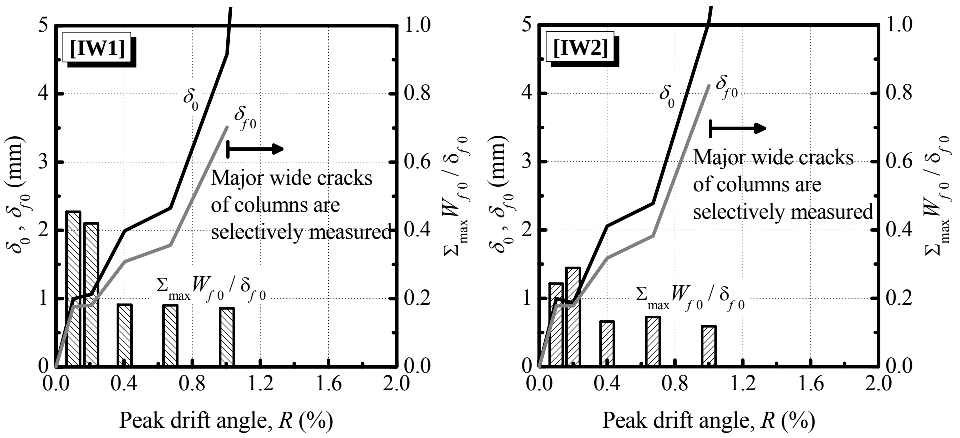

Figure 10: δ_0 , δ_{f0} and $[\Sigma_{\max}W_{f0} / \delta_{f0}]$ vs. peak drift angle R

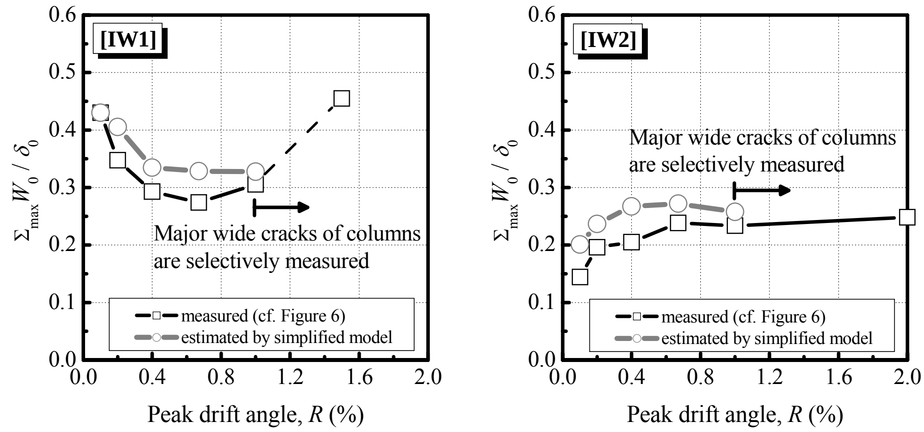

Figure 11: $[\Sigma_{\max}W_0 / \delta_0]$ vs. peak drift angle R (in positive loading)

observed in CB wall based on the ratio [$\Sigma_{max}W_0$ / δ_0]. The residual seismic capacity, therefore, could be evaluated through previously estimated δ_0 if the typical hysteretic characteristics of CB wall infilled frame are given.

4. CONCLUSIONS

Concrete block (CB) infilled RC frames for school buildings in Korea are tested under cyclic loadings, and a simplified model is proposed to investigate the relationship between residual crack widths in CB wall and residual deformation. The results can be summarized as follows.

(1) The measured ratio [$\Sigma_{max}W_0$ / δ_0] for specimens IW1 and IW2 lies approximately in the range of 0.2 to 0.3 before the specimen extensively fails in shear.

(2) Although the ratio above is much smaller than 1.0, a simplified model proposed in this paper considering flexural and shear deformation distribution of columns can rationally reproduce the measured results.

(3) The results described above imply that the residual deformation δ_0 of frames can be estimated from crack widths $\Sigma_{max}W_0$ observed in CB wall based on the ratio [$\Sigma_{max}W_0$ / δ_0]. The residual seismic capacity, therefore, could be evaluated through previously estimated δ_0 if the typical hysteretic characteristics of CB wall infilled frame are given.

ACKNOWLEDGMENT

The research reported herein was performed in cooperation with Professor Waon-Ho Yi of the Kwangwoon University and Dr. Sang-Hoon Oh of RIST (Research Institute of Industrial Science and Technology) in Korea. The authors express their deepest gratitude to all these supports without which the test could not be accomplished.

REFERENCES

The Ministry of Construction and Transportation, 2002. A study on the seismic evaluation and retrofit of low-rise RC buildings in Korea. pp. 113-155.

Masaki Maeda, Masahiro Bunno and Masayuki Nagata, 2000. A study on the damage level estimation of RC buildings based on residual seismic capacity of members. *Proceedings of the Japan Concrete Institute*, Vol. 22, No. 3, pp. 1447-1452.

AIJ(Architectural Institute of Japan), 2004. Guidelines for performance evaluation of earthquake resistant reinforced concrete buildings (Draft) pp. 155-161.